JOURNAL OF THERMOPHYSICS AND HEAT TRANSFER
Vol. 14, No. 3, July–September 2000

Modified YIX Method and Pseudoadaptive Angular Quadrature for Ray Effects Mitigation

Z.-M. Tan* and P.-F. Hsu†
Florida Institute of Technology, Melbourne, Florida 32901
and
S.-H. Wu‡ and C.-Y. Wu§
National Cheng-Kung University, Tainan 701, Taiwan, Republic of China

The ray effects in the YIX method (Hsu, P.-F., Tan, Z.-M., Wu, S.-H., and Wu, C.-Y., "Radiative Heat Transfer in Finite Cylindrical Homogeneous and Nonhomogeneous Scattering Media Exposed to Collimated Radiation," *Numerical Heat Transfer—Part A: Applications*, Vol. 35, No. 6, 1999, pp. 655–679) for computation of radiative heat transfer in a three-dimensional nonhomogeneous participating medium are studied. Remedial methods for the efficient treatment of ray effects are presented. To demonstrate the effectiveness of the methods, ray effects caused by 1) abrupt step changes in the boundary conditions and 2) the stepwise variation of the source function are discussed. In the modified YIX method, the mitigation of the ray effects is achieved by dividing the radiative transfer into emission and scattering components, where the former is solved by numerical integration of the exact integral formulation of the emission components and the latter by the YIX method separately. A pseudoadaptive angular quadrature is implemented in the YIX method. This quadrature uses a different number of angular abscissas in different directions according to the source and the severity of the ray effects. The results by the modified YIX method and a pseudoadaptive angular quadrature method are compared with the solutions obtained by the quadrature method (QM). The QM solution is used as the basis of comparison because of its high-order accuracy.

Nomenclature

A	= area, m^2
a	= absorption coefficient, m^{-1}
$\cos(\hat{\boldsymbol{r}}_1, \hat{\boldsymbol{r}}_2)$	= cosine function with argument is the angle between two vectors $\hat{\boldsymbol{r}}_1$ and $\hat{\boldsymbol{r}}_2$
e	= emissive power, W/m^2
f	= integrand
G	= integrated intensity, W/m^2
I	= radiation intensity, W/m^2 sr
K	= kernel function defined by Eq. (5)
N_v	= number of angular quadrature points in the volume integral
N_w	= number of angular quadrature points in the surface integral
N_x, N_y, N_z	= grid size in each coordinate direction
n	= number of volume elements between $\hat{\boldsymbol{r}}$ and $\hat{\boldsymbol{r}}'$, with $\hat{\boldsymbol{r}}'$ at the boundary
$\hat{\boldsymbol{n}}$	= inward unit normal vector
q	= radiative heat flux, W/m^2
$\hat{\boldsymbol{r}}$	= position vector, m
s	= radiation path length, m
t	= optical distance; Eq. (9)
t_i	= distance quadrature abscissa point in optical coordinate; Eq. (9)
V	= volume, m^3
W_i	= weight of quadrature set
x, y, z	= rectangular coordinates, m
θ	= polar angle, rad
κ	= extinction coefficient, $a + \sigma$, m^{-1}
ξ	= dummy variable
σ	= scattering coefficient, m^{-1}
σ_m	= rms error defined by Eq. (14)
τ	= optical distance defined by Eq. (6)
Φ	= scattering phase function
φ	= azimuthal angle, rad
Ω	= solid angle, sr
ω	= scattering albedo, σ/κ
$\hat{\boldsymbol{\omega}}$	= angular direction unit vector

Subscripts

b	= black body
g	= medium
s	= boundary
$', ''$	= dummy variable

Received 24 May 1999; revision received 6 December 1999; accepted for publication 22 January 2000.

*Visiting Scholar, Mechanical Engineering Program; Associate Professor, Chemical Engineering Research Institute, South China University of Technology, 510641 Guangzhou, People's Republic of China.
†Associate Professor, Mechanical Engineering Program; phsu@fit.edu. Member AIAA.
‡Doctoral Candidate, Department of Mechanical Engineering.
§Professor, Department of Mechanical Engineering.

Introduction

SOLUTIONS to the equations of radiative heat transfer may be found in a number of ways, of which the discrete ordinates method (DOM) has become very commonly used in recent years.[1,2] The DOM is based on a discretized representation of the directional variation of the radiative intensity. Because it may be carried out to any arbitrary order and accuracy, the DOM has been used in many applications, for example, three-dimensional cylinders,[3] nonhomogeneous atmospheres,[4] nonhomogeneous spheres,[5] etc. However, in multidimensional problems, the DOM may suffer from the ray effects. The ray effect is the error caused by the finite number of angular quadrature to represent the angular variation of intensity or its moments. This effect is especially evident when the optical thickness is small and the emissive power in the medium, radiative property distribution, or the incident radiation from the boundary has abrupt variation. The ray effect distorts the solution and needs to be treated carefully. Ray effects have also been observed in other solution methods that use discretized angular quadrature, for example, the discrete transfer method[6] and the YIX method.[7]

Lathrop[8] and Chai et al.[9] presented thorough discussions of the causes of the ray effects. Remedies have been proposed.[10–12] Lewis and Miller[12] suggested several remedies. For example, they discussed a method that could smear out ray effects by using piecewise

continuous approximations to the angular variables. However, for abrupt, stepwise variation, a higher-order interpolation will be needed. This approach would not completely eliminate the ray effect, albeit the approach would reduce its influence to a smaller magnitude. Wu et al.[13] proposed a method to remedy ray effects due to Fresnel boundaries. They improved the solutions by concentrating more discrete ordinates around the critical angles.

More recently, Liou and Wu[14] and Ramankutty and Crosbie[15,16] used a concept similar to Olfe's modified differential approximation[17–19] by splitting the intensity into two components: one contributed by incident radiation and the other by medium emission and scattering. The former can be solved exactly when the boundary condition contains nonsmooth surface emission. The latter is treated by the DOM with a uniform boundary condition. The nonsmooth emission source could cause the ray effects. The technique is explored further in this study by combining the numerical integration of the exact integral formulation of the boundary and medium emission and the solution of the other parts by the YIX method. Because the former treats the boundary and medium emission exactly, the ray effects from stepwise boundary and medium emission sources can be removed. The YIX method is used to handle the scattering component, which is not only less likely to be affected by the ray effect, but tends to smear out the effect if it exists.[10] The approach can be extended to other solution methods.

Another approach is to increase the order of the discretized angular quadrature or discrete ordinates in the directions or regions where the ray effect is obvious.[7] Once implemented, this approach makes it easy to handle the ray effects caused by various situations. The ray effect mitigation depends strongly on the order of the angular quadrature. However, high-order angular quadrature causes long execution times. The execution time increase can be kept to a minimum if an adaptive angular quadrature is used, that is, the high-order quadrature only applies to the regions and directions subjected to the ray effect instead of to the whole computational domain. This approach can handle the ray effects from the sources mentioned as well as those caused by the stepwise radiative property distribution.[7]

This paper focuses on using two different approaches to mitigate the ray effect in a three-dimensional nonhomogeneous participating medium and compares their relative effectiveness. To demonstrate the efficiency of the remedial methods, radiative heat transfer in a cube with stepwise emissive power in the medium and at the boundary is examined. Although the posed problems studied here are artificial, they do resemble practical situations in turbulent flames and combustion systems.

Mathematical Description of the Problem

The equation for variation of the radiative intensity in an absorbing, emitting, and scattering medium along an arbitrary direction is

$$\frac{\mathrm{d}I(\hat{\boldsymbol{r}},\hat{\boldsymbol{\omega}})}{\mathrm{d}s} = -\kappa I(\hat{\boldsymbol{r}},\hat{\boldsymbol{\omega}}) + aI_b(\hat{\boldsymbol{r}}) + \frac{\sigma}{4\pi}\int_{\Omega'=4\pi} I(\hat{\boldsymbol{r}},\hat{\boldsymbol{\omega}}')\Phi(\hat{\boldsymbol{\omega}}',\hat{\boldsymbol{\omega}})\,\mathrm{d}\Omega' \tag{1}$$

In this study, scattering is supposed to be isotropic, in which case

$$\Phi(\hat{\boldsymbol{\omega}}',\hat{\boldsymbol{\omega}}) = 1 \tag{2}$$

The integral formulation of radiative transfer in a three-dimensional, gray, absorbing, emitting, and scattering medium with a black boundary can be obtained through the integral formulations developed by Crosbie and Schrenker,[20] Tan,[21] or Wu et al.[22] Black surfaces are assumed because the ray effect then will be most evident. The integrated intensity at any position in the volume is

$$G(\hat{\boldsymbol{r}}) = \iint K(\hat{\boldsymbol{r}},\hat{\boldsymbol{r}}')e_s(\hat{\boldsymbol{r}}')\cos(\hat{\boldsymbol{r}}-\hat{\boldsymbol{r}}',\hat{\boldsymbol{n}})\,\mathrm{d}A(\hat{\boldsymbol{r}}') + \iiint K(\hat{\boldsymbol{r}},\hat{\boldsymbol{r}}')a(\hat{\boldsymbol{r}}')e_g(\hat{\boldsymbol{r}}')\,\mathrm{d}V(\hat{\boldsymbol{r}}') + \iiint K(\hat{\boldsymbol{r}},\hat{\boldsymbol{r}}')\sigma(\hat{\boldsymbol{r}}')\frac{G(\hat{\boldsymbol{r}}')}{4}\,\mathrm{d}V(\hat{\boldsymbol{r}}') \tag{3}$$

where

$$G(\hat{\boldsymbol{r}}) = \int_{\Omega'=4\pi} I(\hat{\boldsymbol{r}},\hat{\boldsymbol{\omega}}')\,\mathrm{d}\Omega' \tag{4}$$

The first or the second term on the right-hand side of Eq. (3) is called the driving term (or component) in this work depending on the given conditions. The kernel K is defined by

$$K(\hat{\boldsymbol{r}},\hat{\boldsymbol{r}}') = \frac{\exp[-\tau(\hat{\boldsymbol{r}},\hat{\boldsymbol{r}}')]}{\pi|\hat{\boldsymbol{r}}-\hat{\boldsymbol{r}}'|^2} \tag{5}$$

and $\hat{\boldsymbol{\omega}}$ is a unit vector in the $\hat{\boldsymbol{r}}'$–$\hat{\boldsymbol{r}}$ direction. The optical distance is

$$\tau(\hat{\boldsymbol{r}},\hat{\boldsymbol{r}}') = \int_{\hat{r}'}^{\hat{r}} \kappa(\hat{\boldsymbol{r}}'')\,\mathrm{d}|\hat{\boldsymbol{r}}''| = \int_0^1 \kappa[\hat{\boldsymbol{r}}'+\xi(\hat{\boldsymbol{r}}-\hat{\boldsymbol{r}}')]\cdot|\hat{\boldsymbol{r}}-\hat{\boldsymbol{r}}'|\,\mathrm{d}\xi \tag{6}$$

The radiative heat flux in the medium and at the surface can be expressed in forms similar to that of Eq. (3).[7,21] Once the integrated intensity is determined, the radiative heat flux in the medium and at the surface are readily calculated.

Numerical Methods

Quadrature Method

In this method,[22] integrated intensity and heat flux are expressed in integral forms in terms of the moments of intensity. Applying the product Gaussian–Legendre quadrature formula to the approximation of volume integrals, the integral equations can be transformed into a set of algebraic equations. Numerical results of the moments of intensity at the quadrature nodes are obtained by solving the algebraic equations.

The success of the quadrature method (QM) depends on the identification of all discontinuities, including the abrupt change in the boundary condition or in the source function in the medium. QM applies numerical quadrature to each integration subinterval over which the integrand has smooth variation. Therefore, to solve cases 2a and 2b described in a later section, a composite quadrature is adapted to approximate the z-direction integration over the domain of $[-0.5, 0.5]$ because the medium emissive power has a discontinuity at the $z=0$ interface. For such an integral, a composite Gaussian–Lagendre quadrature is used. One is used for the subinterval of $[-0.5, 0]$ and the other for $[0, 0.5]$.

Frequently, it is necessary to find the moments of intensity on the enclosure surfaces or at interior points that do not match any of the Gaussian quadrature nodes. Although the variation of the scattering parts is smooth, that of the driving terms is drastic, especially in the region around the intersection lines or the interfaces with the discontinuities and/or the nonsmooth variations from the source function or the boundary conditions. Thus, instead of interpolating the moments of intensity from the results of the quadrature nodes, we find the driving terms from direct numerical integration and evaluate only the scattering parts by Lagrange interpolation (or extrapolation) from the results of the quadrature nodes.

The QM method does not produce the ray effect that comes from the angular quadrature because the discontinuities and/or the nonsmooth variations from the source function or the boundary condition are properly accounted for. It generates highly accurate solutions.[22] Therefore, the QM solutions are used as benchmarks for comparison.

YIX Method

In this method, the volume and surface integrations on the right side of Eq. (3) are constructed as follows:

$$\iiint K(\hat{\boldsymbol{r}},\hat{\boldsymbol{r}}')F(\hat{\boldsymbol{r}}')\,\mathrm{d}V(\hat{\boldsymbol{r}}') = \int_0^{4\pi}\frac{\mathrm{d}\Omega}{\pi}\int_0^{R(\hat{r},\hat{\omega})}\exp\left[-\int_0^t \kappa(\hat{\boldsymbol{r}}+\hat{\boldsymbol{\omega}}t')\,\mathrm{d}t'\right]F(\hat{\boldsymbol{r}}+\hat{\boldsymbol{\omega}}t)\,\mathrm{d}t \approx \sum_{i=1}^{N_v} W_i\int_0^{R(\hat{r},\hat{\omega}_i)}\exp\left[-\int_0^t \kappa(\hat{\boldsymbol{r}}+\hat{\boldsymbol{\omega}}_i t')\,\mathrm{d}t'\right]F(\hat{\boldsymbol{r}}+\hat{\boldsymbol{\omega}}_i t)\,\mathrm{d}t \tag{7}$$

$$\iint K(\hat{\boldsymbol{r}}, \hat{\boldsymbol{r}}') F(\hat{\boldsymbol{r}}') \cos(\hat{\boldsymbol{r}} - \hat{\boldsymbol{r}}', \hat{\boldsymbol{n}})\, \mathrm{d}A(\hat{\boldsymbol{r}}')$$

$$= \int_0^{4\pi} \exp\left[- \int_0^{R(\hat{r}, \hat{\omega})} \kappa(\hat{\boldsymbol{r}} + \hat{\boldsymbol{\omega}} t')\, \mathrm{d}t' \right] F(\hat{\boldsymbol{r}} + \hat{\boldsymbol{\omega}} R) \frac{\mathrm{d}\Omega}{\pi}$$

$$\approx \sum_{i=1}^{N_w} W_i \exp\left[- \int_0^{R(\hat{r}, \hat{\omega}_i)} \kappa(\hat{\boldsymbol{r}} + \hat{\boldsymbol{\omega}}_i t')\, \mathrm{d}t' \right] F(\hat{\boldsymbol{r}} + \hat{\boldsymbol{\omega}}_i R) \quad (8)$$

where $R(\hat{\boldsymbol{r}}, \hat{\boldsymbol{\omega}})$ is the length of a beam emitted from $\hat{\boldsymbol{r}}$ in the $\hat{\boldsymbol{\omega}}$ direction and striking the nearest boundary. N_v and N_w are the numbers of angular quadrature points of the volume and boundary integrals. They depend on the order of the angular quadrature sets used. The distance integral in Eq. (7) is evaluated by unevenly spaced integration points along the angular directions:

$$\int_0^L K(t) f(t)\, \mathrm{d}t = \sum_{i=1}^{n} \int_{t_{i-1}}^{t_i} K(t) f(t)\, \mathrm{d}t + \int_{t_n}^{L} K(t) f(t)\, \mathrm{d}t$$

$$= \lambda \left[f(0) + \sum_{i=1}^{n-1} f(t_i) \right] + [P_{n+1} + L Q_{n+1}] f(t_n) \quad (9)$$

where $f(t) \equiv f[\hat{\boldsymbol{r}}', (t)]$ is the unknown at $\hat{\boldsymbol{r}}'$ in the computational domain, which is divided into $N_x N_y N_z$ volumes and is found by piecewise constant interpolation. P, L, Q, and t_i are quadrature constants that depend on the kernel function (K) and the accuracy requirements.[23]

The choice of angular quadrature direction and the number of angular quadrature points (or angular abscissas) are arbitrary for this method. The following three schemes are used for comparison.

S16 (Designated YIX-S16)

The discrete ordinates set Sn is used in the angular quadrature. To maintain the same order of accuracy in angular integration at volume and boundary elements, the fully symmetric discrete ordinates and weight sets are usually used. The symmetric discrete ordinates direction sets S16 with a total of 288 angular quadrature points[24] were adopted. For the two types of problem considered, it is found that symmetric discrete ordinates sets are inadequate to handle the ray effect. Other angular quadrature sets, for example, Tn (Ref. 25), have been used and are also subject to the ray effect. Hence, different angular quadrature schemes (which even then may not satisfy the level symmetric moment-matching requirement) are needed for more quadrature points.[2]

Simpson's Rule (Designated YIX-Sp)

For the integral over the solid angle in Eq. (7),

$$\int_{4\pi}\int f(\theta, \varphi) \sin\theta\, \mathrm{d}\theta\, \mathrm{d}\varphi = \int_0^{2\pi} \left[\int_{-1}^{1} f(\theta, \varphi)\, \mathrm{d}(-\cos\theta) \right] \mathrm{d}\varphi \quad (10)$$

Both integration ranges $[0, 2\pi]$ and $[-1, 1]$ are divided into $2m$ subintervals of equal width. Suppose $\cos\theta_i = (i - m)/m$, the integral

$$\int_{-1}^{1} f(\theta, \varphi)\, \mathrm{d}(-\cos\theta)$$

can be carried out according to Simpson's one-third rule:

$$\int_{-1}^{1} f(x)\, \mathrm{d}x = \sum_{0}^{2m-1} \int_{x_1}^{x_{i+1}} f(x)\, \mathrm{d}x$$

$$= \frac{\Delta x}{3} [f_0 + 4f_1 + \cdots + 2f_{2m-2} + 4f_{2m-1} + f_{2m}] \quad (11)$$

The total number of angular quadrature points is $N_v = 2m(2m + 1)$, which may be any desired value.

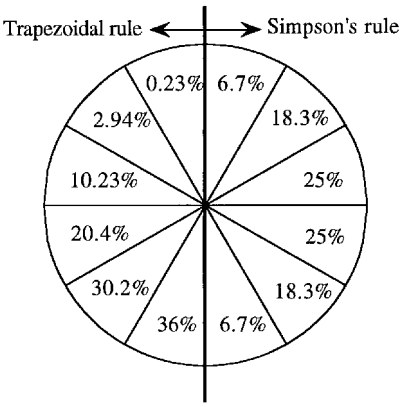

Fig. 1 Pseudoadaptive angular quadrature: comparison of percentage of angular rays, using adaptive trapezoidal rule and Simpson's rule.

Pseudoadaptive Angular Quadrature (Designated YIX-A)

Because the ray effects are due to the limited number of angular quadrature points in certain directions, it is reasonable to increase the number of angular quadrature points only in those directions. The application of adaptive angular quadrature is based on this consideration by using different numbers of angular quadrature points in different regions and in different directions according to the cause and the severity of the ray effects. The advantage of an adaptive procedure is to mitigate the ray effects as much as possible and at the same time hold the increase in computational time to a minimum. For the present study, let

$$\cos\theta_i = x_i = (1/m)\left[\left(2m - \sqrt{4m^2 - i^2} \right) - 1 \right] \quad (12)$$

The integral

$$\int_{-1}^{1} f(\theta, \varphi)\, \mathrm{d}(-\cos\theta)$$

can be carried out according to the trapezoidal rule:

$$\int_{-1}^{1} f(x)\, \mathrm{d}x = \sum_{1}^{2m} \int_{x_{i-1}}^{x_i} f(x)\, \mathrm{d}x$$

$$= \frac{1}{2} [\Delta x_1 f_0 + \cdots + (\Delta x_{2m-1} + \Delta x_{2m}) f_{2m-1} + \Delta x_{2m} f_{2m}] \quad (13)$$

where $\Delta x_i = x_i - x_{i-1} = \{ \sqrt{[4m^2 - (i-1)^2]} - \sqrt{[4m^2 - i^2]} \}/m$, $i = 1, 2, \ldots, 2m$. The total number of angular quadrature points is $N_v = 2m(2m + 1)$. The discretization of Eq. (12) allows the angular quadrature to concentrate the abscissa around the x_m direction (Fig. 1). The current scheme is called pseudoadaptive. A fully adaptive scheme adjusts the angular abscissa during each iteration, and the required N_v is very small. An adaptive scheme can either adjust the abscissa position and weight or add extra abscissa values on the detection of the ray effect. The implementation needs an appropriate data structure and is left as a future task.

Modified YIX Method

The modified YIX method is a modification of the YIX method that treats ray effects by dividing the integration in Eq. (3) into boundary emission, medium emission, and scattering components. Depending on whether the ray effects are caused by the abrupt change of emissive power in the medium or at the boundary, the corresponding emission term is obtained by numerical integration of the exact integral formulation in a way similar to that in the QM. The other emission term and the scattering term are solved by the YIX method.

Results and Discussion

To demonstrate the application of the methods, radiative heat transfer in a three-dimensional nonhomogeneous participating medium is studied. The cases selected are 1) a unit cube with all

Table 1 Conditions for the cases studied

Case	Extinction coefficient distribution	Emissive power in the medium	Emissive power at the boundary	Scattering albedo
1a	$\kappa = 0.1 + 0.9[(1-4x^2)\times(1-4y^2)(1-4z^2)]^2$	$e_b = 0$	$e_{s1} = e_{s2} = e_{s3} = e_{s4} = e_{s5} = 0$, $e_{s6} = 1$	$\omega = 1, 0.5, 0.1$
1b	$\kappa = 0.1, 1, 5$	$e_b = 0$	$e_{s1} = e_{s2} = e_{s3} = e_{s4} = e_{s5} = 0$, $e_{s6} = 1$	$\omega = 1$
2a	$\kappa = 1$	$e_b = 0.5, 0 < z < 0.5$; $e_b = 1, -0.5 < z < 0$	$e_s = 0$	$\omega = 0.9, 0.5, 0.1$
2b	$\kappa = 1$	$e_b = 0.1, 0 < z < 0.5$; $e_b = 1, -0.5 < z < 0$	$e_s = 0$	$\omega = 0.9, 0.5, 0.1$

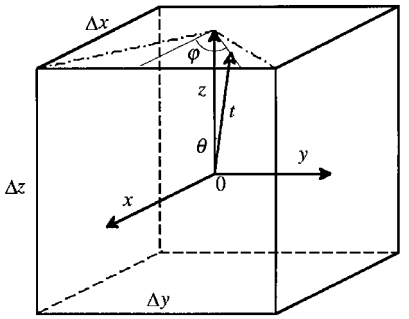

Fig. 2 Geometry of a volume element integration.

black surfaces exposed to uniform diffuse radiation from its bottom surface $z = -0.5$, with the other five surfaces cold and an extinction coefficient distribution in the medium $\kappa(x, y, z) = 0.1 + 0.9[(1-4x^2)(1-4y^2)(1-4z^2)]^2$ or a constant extinction coefficient of $\kappa = 0.1$, 1, or 5 and 2) a unit cube with a constant extinction coefficient $\kappa = 1$, six cold and black surfaces, and a step change for the emissive power in the medium: $e_{b1} = 0.5$ or 0.1 at $0 \le z \le 0.5$ and $e_{b2} = 1$ at $-0.5 \le z \le 0$. The first case produces ray effects caused by the abrupt change in the boundary conditions, that is, the juxtaposition of hot and cold surfaces. The second case produces ray effects caused by the nonuniform distribution of the source function. The latter case is frequently encountered in turbulent flames and fires and in some industrial applications.[26] The geometry of the medium and coordinates are similar to that in Fig. 2, and the conditions for the cases are listed in Table 1. The results are normalized with respect to the emissive power of the bottom surface (case 1) or the emissive power of the region at $-0.5 \le z \le 0$ (case 2). The G function and the heat flux depend on the position within the enclosure. In the rectangular coordinate system, the dependence is expressed in terms of (x, y, z), as shown in Figs. 3–13.

All calculations are carried out by dividing the medium into $N_x N_y N_z$ volume elements and $2(N_x N_y + N_y N_z + N_z N_x)$ surface elements. The distribution of the integrated intensity in the medium and the heat flux at the boundary are presumed to be piecewise continuous for all of the methods discussed. The QM results presented are interpolated values at the nodes used in the other methods. The YIX method uses $t_1 = 0.001$, where t_1 represents the first integration point in the optical thickness dimension. The run times of case 1 with $\omega = 0.1$ are 7860 s for QM, 4647 s for modified YIX, and 8168 s for YIX-A. Both modified YIX and YIX-A were applied with $N_v = 1952$. The computational time of YIX-A is proportional to N_v. All calculations were performed on a Pentium-Pro 200-MHz personal computer.

Case 1: Ray Effect Caused by the Stepwise Boundary Condition

Figure 3 shows the integrated intensity along the centerline $x = y = 0$ in the medium with scattering albedo $\omega = 0.1$ for case 1a. The medium is divided into $17 \times 17 \times 17 = 4913$ volume elements and the surface into $6 \times (17 \times 17) = 1734$ surface elements. The QM uses the grid size as the interpolation points to obtain the solution values for comparison. It is seen that the ray effect appears

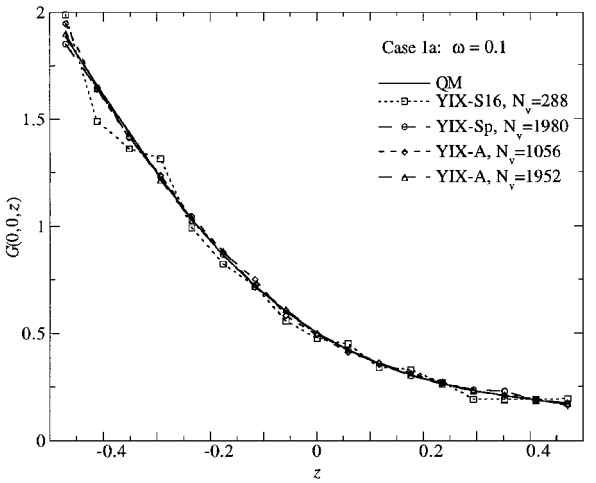

Fig. 3 Influence of the ray effect on the integrated intensity along the centerline $x = y = 0$ in a cubic medium with a hot black bottom.

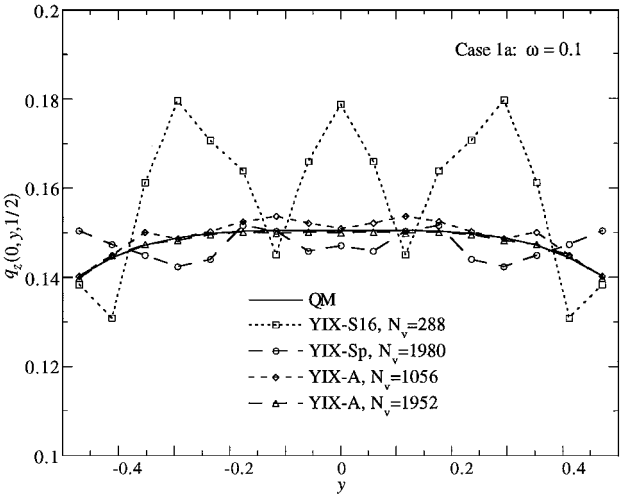

Fig. 4 Influence of the ray effect on heat flux at the top of a cubic medium with a hot black bottom.

in the YIX-S16 solution of the G distribution. The YIX-Sp solution with 1980 angular quadrature points and the YIX-A solution with 1056 angular quadrature points show some difference from the QM solution. The former has 2.5% rms difference and the latter 0.08% rms difference. The YIX-A solution with 1952 angular quadrature points is very close to the QM solution with only 0.02% rms difference. The ray effects are even more obvious, as shown in Fig. 4 by the heat fluxes at the top surface. Because this surface is the farthest from the bottom emitting surface, the chance of a particular angular abscissa misrepresenting either hot or cold surface is greater. Therefore, larger error occurs. In general, the magnitude of the error depends on combining the effects of the extinction

coefficient distribution, the albedo, the distance between the top and bottom surfaces, and the relative orientation of the two surfaces.

Figure 4 presents the heat flux distribution at the top surface of a medium with scattering albedo $\omega = 0.1$ for case 1a. The ray effect is evident in the YIX-S16 solution with 288 angular quadrature points. Because the ray effect is caused by the approximation of a limited number of angular quadrature points (in this case, a set of discrete ordinates), it is expected to be mitigated by increasing the number of angular directions or N_v. Theoretically, there is no limit to the maximum number of discrete ordinates, but physically unrealistic negative weights are encountered for very high-order level symmetric discrete ordinates sets. Therefore, angular quadrature schemes other than the conventional *Sn* sets are recommended where negative weights would not occur for any number of discretized angular directions. The results obtained by YIX-Sp with 1980 angular Simpson quadrature points show a great improvement in ray effects compared with those of the YIX-S16 with $N_v = 288$. However, the computational time of YIX-Sp is much longer (the computational time is proportional to N_v), and furthermore, the ray effect is still evident. This suggests the use of a more flexible angular quadrature scheme in which the ray effect can be mitigated as much as possible and at the same time the increase of the computational time is kept to a minimum. The adaptive angular quadrature is such a scheme, where the angular quadrature points may be placed in any manner advantageous to the solution of the problem at hand. YIX-A is a pseudoadaptive quadrature method. It is apparent that, by applying the limited adaptive angular quadrature in the YIX-A with $N_v = 1056$, the solutions are more accurate than those of the YIX-Sp with $N_v = 1980$. The solution of the YIX-A with $N_v = 1952$ is very close to the QM solution. Unless specified otherwise, all YIX-A calculations were done with $N_v = 1952$. The adaptive angular quadrature scheme mitigates the ray effect more effectively than the YIX-Sp scheme.

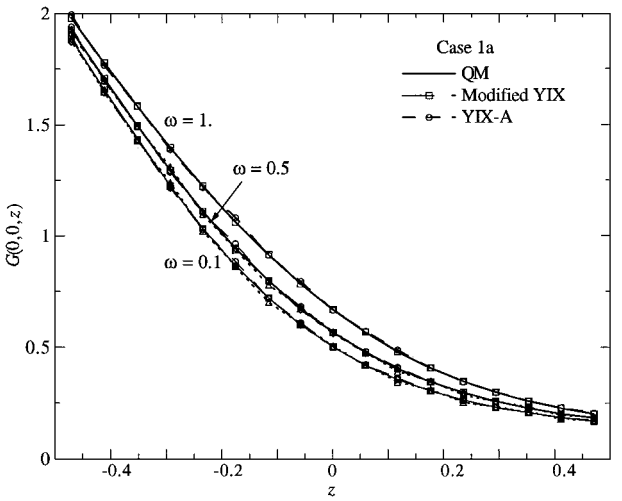

Fig. 5 Integrated intensity along the centerline $x = y = 0$ in a cubic medium with a hot black bottom.

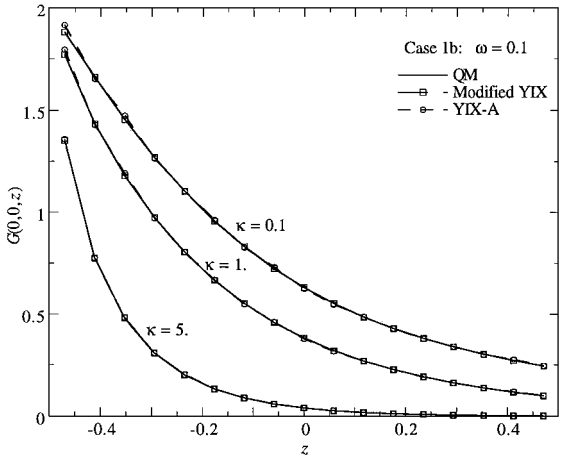

Fig. 6 Integrated intensity along the centerline $x = y = 0$ in a cubic medium with a hot black bottom.

Figures 5 and 6 compare the integrated intensity distributions obtained by the QM and the remedial methods for cases 1a and 1b. The number of angular quadrature points for the modified YIX is 1952, and that for the YIX-A is 1980. The angular quadrature points are set to be almost the same for convenience of comparison. For all three situations with different scattering albedo, the results of the modified YIX are in very good agreement with the QM results. In the modified YIX method, the integrated intensity is divided into the component caused by the incident radiation from the bottom surface and the component caused by the scattering in the medium; the former is found by numerical integraion similar to the QM, and the latter is solved by the YIX method. Because the QM is expected to give highly accurate results, it shows that ray effects in the other solutions are mainly caused by the incident radiation from the bottom surface for this case. The results by the YIX-A still show small deviations from the QM solutions because of the influence of the angular quadrature.

In this case, the emissive power of the medium $e_g = 0$, and the volume integration in Eq. (3) only includes scattering effect. Because scattering is simply a redirection process for part of the incoming intensity, the integrated intensity depends mainly on the incident radiation from the bottom. Although the integrated intensity increases with an increase in scattering albedo, the change is small for case 1a (Fig. 5). For a fixed scattering albedo, the integrated intensity decreases with the increase of extinction coefficient (or optical thickness) due to stronger attenuation for case 1b (Fig. 6).

Cases 1a and 1b heat fluxes at the top surface $x = 0$ and $z = 0.5$ are plotted in Figs. 7 and 8, respectively. The heat flux distributions include the contributions from both the incident radiation of the bottom and the scattering of the medium. The heat flux at the top surface increases with an increase in scattering albedo at a fixed extinction coefficient distribution for case 1a in Fig. 7. It decreases with an increase in extinction coefficient at constant scattering albedo for case 1b in Fig. 8. The ray effect can be seen from the solutions by the YIX-A method at $\kappa = 0.1$ in Fig. 8 because the ray effect is most evident when the optical thickness is small.

To conduct quantitative error analysis, the values of the heat flux at the top surface $x = 0$ and $z = 0.5$ for case 1a are tabulated (Table 2). The rms error with respect to the QM results is presented. The rms error is calculated according to the following relation:

$$\sigma_m = \sqrt{\sum_1^n \left(\frac{q - q_{\mathrm{QM}}}{q_{\mathrm{QM}}}\right)^2 \Big/ n} \tag{14}$$

where the QM solution is used as the basis for comparison. The error numbers reported in Table 2 are based on the comparison of all surface elements. It can be seen that the rms error for modified YIX is the smallest. The rms error for the YIX-A is greater than that for modified YIX. This is because the results obtained by YIX-A

Table 2 Heat fluxes through top surface ($x = 0, z = 0.5$) and their standard deviations (case 1a, $\omega = 0.1$)

y	QM	Modified YIX	YIX-A	YIX-Sp	YIX-S16
0.00000	0.15043	0.15046	0.14993	0.14703	0.17874
0.05882	0.15044	0.15046	0.15014	0.14586	0.16593
0.11675	0.15041	0.15044	0.14984	0.15027	0.14502
0.17647	0.15025	0.15028	0.15013	0.15158	0.16385
0.23529	0.14980	0.14982	0.14947	0.14405	0.17066
0.29412	0.14883	0.14886	0.14822	0.14235	0.17959
0.35294	0.14711	0.14713	0.14735	0.14493	0.16124
0.41176	0.14435	0.14437	0.14488	0.14736	0.13085
0.47059	0.14030	0.14032	0.13975	0.15036	0.13840
σ_m (%)	0.00	0.015	0.56	5.06	12.8

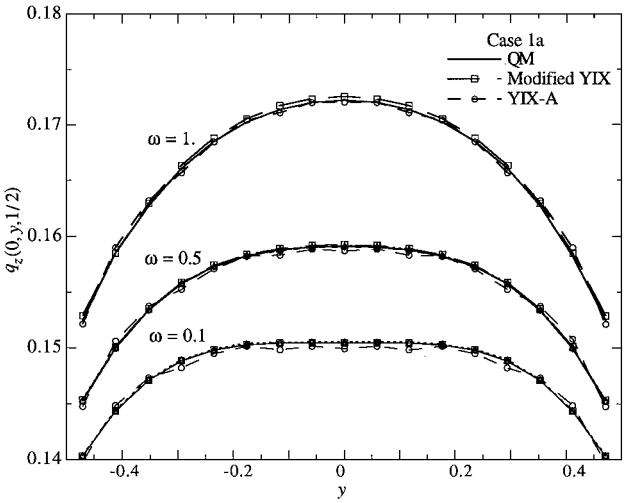

Fig. 7 Heat flux at the top of a cubic medium with a hot black bottom.

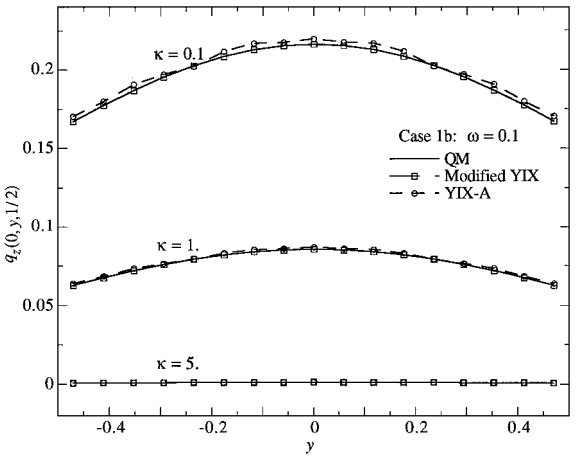

Fig. 8 Heat flux at the top of a cubic medium with a hot black bottom.

depend on the order of the angular quadrature. The rms error for YIX-Sp is at least one or two orders of magnitude larger than those of the modified YIX and YIX-A. The rms error for YIX-S16 is the greatest.

Case 2: Ray Effect Caused by a Stepwise Emissive Power in the Medium

For this case, two situations are considered: the emissive power of the medium $e_b = 0.5$ or 0.1, in the upper half, and $e_b = 1$, in the lower half. The element number in the z coordinate direction is chosen to be even, considering that the emissive power has a step change in the middle of the medium, that is, $z = 0$. The medium is divided into $16 \times 16 \times 16 = 4096$ volume elements and the surface is divided into $6 \times (16 \times 16) = 1536$ elements for the convenience of calculation and comparison.

Cases 2a and 2b YIX-S16 solutions for the heat flux at the top surface ($x = \frac{1}{32}$ and $z = 0.5$) with the scattering albedo $\omega = 0.1$ are compared with the QM solutions in Fig. 9. The heat fluxes from YIX-S16 deviate significantly from the QM results at $y = \pm 0.35$ due to the ray effect. The absolute error is 0.0072, and the relative error is 2.76% for case 2a, whereas errors for case 2b are 0.012 and 10.7%, respectively. Because the only difference between cases 2a and 2b is the extent of the step change in the emissive power of the medium, this demonstrates that the greater this change, the stronger the ray effect.

Figures 10 and 11 show the integrated intensity along the line $x = y = \frac{1}{32}$ in the medium with different scattering albedo for cases 2a and 2b. In both cases, the medium has a uniform extinction coefficient $\kappa = 1$. The volume integration in Eq. (3) includes the

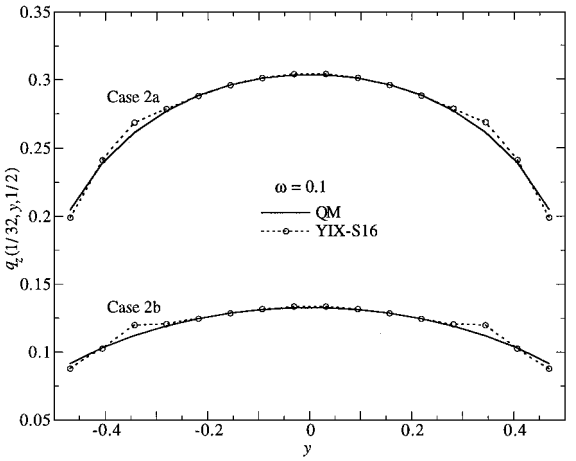

Fig. 9 Influence of the ray effect on heat flux at the top of a cubic medium with a discontinuous distribution of source function.

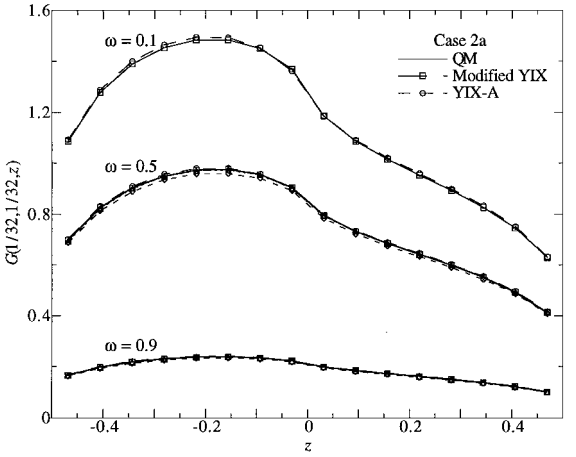

Fig. 10 Integrated intensity along the line $x = y = \frac{1}{32}$ in a cubic medium with a discontinuous distribution of source function.

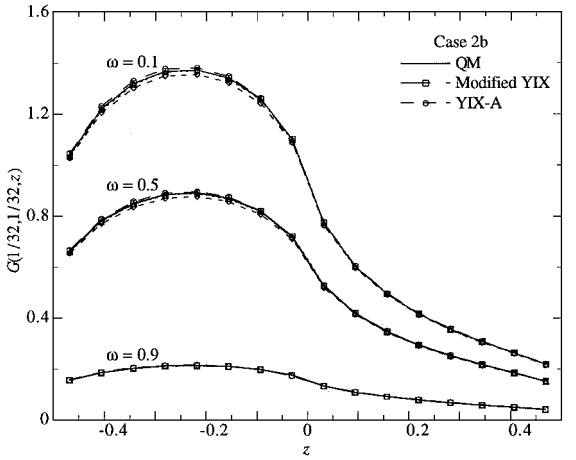

Fig. 11 Integrated intensity along the line $x = y = \frac{1}{32}$ in a cubic medium with a discontinuous distribution of source function.

contributions from both emission and scattering of the medium. The medium emission term is the driving source of the radiative transfer. This means the integrated intensity depends strongly on the emission of the medium for this case. However, the contributions from both emission and scattering are controlled by the scattering albedo. As the scattering albedo increases, the contribution from the emission decreases, as does the ray effect, if it exists in the solution methods. Therefore, the integrated intensity decreases with an increase in scattering albedo. By comparing Figs. 10 and 11, one can see that the integrated intensity values for case 2a are greater than those for

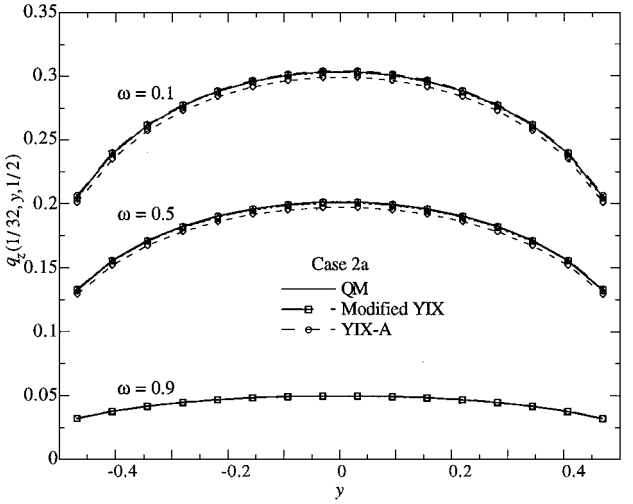

Fig. 12 Heat flux at the top of a cubic medium with a discontinuous distribution of source function.

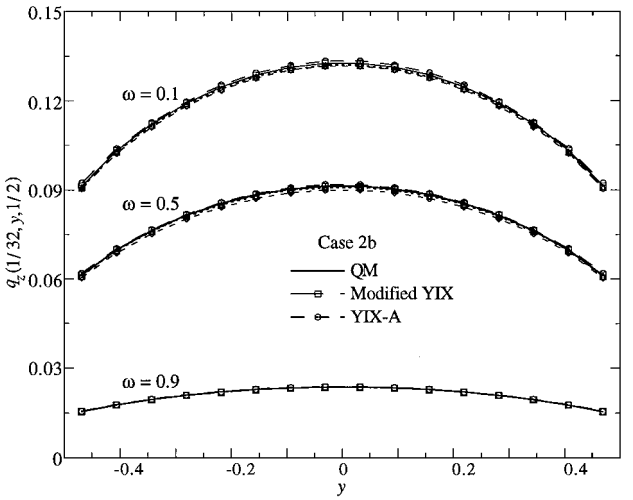

Fig. 13 Heat flux at the top of a cubic medium with a discontinuous distribution of source function.

case 2b. This is because the emissive power in the upper part of the medium for case 2a is greater than for case 2b.

Among the remedial calculation methods, the modified YIX solution has very good accuracy. The YIX-A solution still show small deviations from the QM solution due to the influence of angular quadrature points. The increase of N_y or a better placement of angular quadrature points will improve the solution accuracy. Figures 12 and 13 show the heat flux for cases 2a and 2b. They exhibit the same error trend as in the results of the integrated intensity distribution. Note that the ray effect will be less evident in optically thin medium due to the very weak medium emission. This is opposite to that shown in Fig. 8 of case 1b.

Conclusions

Abrupt variation of the boundary conditions or of the source function in the medium can lead to ray effects in methods relying on discrete angular quadrature. Mitigation of these effects is achieved by 1) splitting the radiative intensity into the driving (emission or irradiation) and scattering components and then computing the former by numerical integration of the exact integral formulation and solving the latter by the YIX method or by 2) using adaptive angular quadrature, concentrating any desired quadrature points in the directions with step changes in emissive power. Our results show that the first approach is consistently more effective than the second, but the second is much easier to implement than the first. Both methods are more effective than simply increasing the angular quadrature order, as shown by the YIX-Sp and YIX-S16 results.

Acknowledgments

This work was supported by the U.S. National Science Foundation through Grant INT-9512131 and the National Science Council of the Republic of China in Taiwan through Grant NSC85-2212-E006-021.

References

[1]Truelove, J. S., "Three-Dimensional Radiation in Absorbing-Emitting-Scattering Media Using the Discrete-Ordinates Approximation," *Journal of Quantitative Spectroscopy and Radiative Transfer*, Vol. 39, No. 1, 1988, pp. 27–31.

[2]Fiveland, W. A., "Three-Dimensional Radiative Heat-Transfer Solutions by the Discrete-Ordinates Method," *Journal of Thermodynamics and Heat Transfer*, Vol. 2, No. 4, 1988, pp. 309–316.

[3]Jamaluddian, A. S., and Smith, P. J., "Discrete-Ordinates Solution of Radiative Transfer Equation in Nonaxisymmetric Cylindrical Enclosures," *Journal of Thermophysics and Heat Transfer*, Vol. 6, No. 2, 1992, pp. 242–245.

[4]Stamnes, K., Tsay, S.-C., Wiscombe, W. J., and Jayaweera, K., "Numerically Stable Algorithm for Discrete-Ordinate-Method Radiative Transfer in Multiple Scattering and Emitting Layered Media," *Applied Optics*, Vol. 27, No. 12, 1988, pp. 2502–2509.

[5]Tsai, J. R., Ozisik, M. N., and Santarelli, F., "Radiation in Spherical Symmetry with Anisotropic Scattering and Variable Properties," *Journal of Quantitative Spectroscopy and Radiative Transfer*, Vol. 42, No. 3, 1989, pp. 187–199.

[6]Malalasekera, W. M. G., and James, E. H., "Calculation of Radiative Heat Transfer in Three-Dimensional Complex Geometries," *National Heat Transfer Conference*, HTD-Vol. 315, American Society of Mechanical Engineers, Fairfield, NJ, 1995, pp. 53–61.

[7]Hsu, P.-F., Tan, Z.-M., Wu, S.-H., and Wu, C.-Y., "Radiative Heat Transfer in Finite Cylindrical Homogeneous and Nonhomogeneous Scattering Media Exposed to Collimated Radiation," *Numerical Heat Transfer—Part A: Applications*, Vol. 35, No. 6, 1999, pp. 655–679.

[8]Lathrop, K. D., "Ray Effects in Discrete Ordinates Equations," *Nuclear Science and Engineering*, Vol. 32, 1968, pp. 357–369.

[9]Chai, J. C., Lee, H. S., and Patankar, S. V., "Ray Effect and False Scattering in the Discrete Ordinates Method," *Numerical Heat Transfer—Part B: Fundamentals*, Vol. 24, No. 4, 1993, pp. 373–389.

[10]Lathrop, K. D., "Remedies for Ray Effects," *Nuclear Science and Engineering*, Vol. 45, 1971, pp. 255–268.

[11]Briggs, L. L., Miller, W. F., and Lewis, E. E., "Ray-Effect Mitigation in Discrete Ordinate-Like Angular Finite Element Approximations in Neutron Transport," *Nuclear Science and Engineering*, Vol. 57, 1975, pp. 205–217.

[12]Lewis, E. E., and Miller, W. F., Jr., *Computational Methods of Neutron Transport*, Wiley, New York, 1984, Chap. 4.

[13]Wu, C.-Y., Liou, B.-T., and Liou, J.-H., "Discrete-Ordinate Solutions for Radiative Transfer in a Scattering Medium with Fresnel Boundaries," *Proceedings of the 10th International Heat Transfer Conference*, Vol. 2, Taylor and Francis, Bristol, PA, 1994, pp. 159–164.

[14]Liou, B.-T., and Wu, C.-Y., "Ray Effects in the Discrete-Ordinate Solution for Surface Radiation Exchange," *Heat and Mass Transfer*, Vol. 32, No. 4, 1997, pp. 271–275.

[15]Ramankutty, M. A., and Crosbie, A. L., "Modified Discrete-Ordinates Solution of Radiative Transfer in Three-Dimensional Rectangular Enclosures," *Journal of Quantitative Spectroscopy and Radiative Transfer*, Vol. 60, No. 1, 1998, pp. 103–134.

[16]Ramankutty, M. A., and Crosbie, A. L., "Modified Discrete-Ordinates Solution of Radiative Transfer in Two-Dimensional Rectangular Enclosures," *Journal of Quantitative Spectroscopy and Radiative Transfer*, Vol. 57, No. 1, 1997, pp. 107–140.

[17]Wu, C.-Y., Sutton, W. H., and Love, T. J., "Successive Improvement of the Modified Differential Approximation in Radiative Heat Transfer," *Journal of Thermophysics and Heat Transfer*, Vol. 1, No. 4, 1987, pp. 296–300.

[18]Modest, M. F., "The Modified Differential Approximation for Radiative Transfer in General Three-Dimensional Media," *Journal of Thermophysics and Heat Transfer*, Vol. 3, No. 3, 1989, pp. 283–288.

[19]Olfe, D. B., "Radiative Equilibrium of a Gray Medium Bounded by Nonisothermal Walls," *Thermophysics: Applications to Thermal Design of Spacecraft*, edited by J. T. Bevans, Vol. 23, Progress in Astronautics and Aeronautics, AIAA, New York, 1970, pp. 295–317.

[20]Crosbie, A. L., and Schrenker, R. G., "Exact Expression for Radiative Transfer in a Three-Dimensional Rectangular Geometry," *Journal of Quantitative Spectroscopy and Radiative Transfer*, Vol. 28, No. 6, 1982, pp. 507–526.

[21]Tan, Z., "Radiative Heat Transfer in Multidimensional Emitting, Absorbing, and Anisotropic Scattering Media—Mathematical Formulation and

Numerical Method," *Journal of Heat Transfer*, Vol. 111, No. 1, 1989, pp. 141–47.

[22]Wu, S.-H., Wu, C.-Y., and Hsu, P.-F., "Solution of Radiative Heat Transfer in Nonhomogeneous Participating Media Using the Quadrature Method," *1996 ASME International Mechanical Engineering Congress and Exposition*, HTD-Vol. 332, American Society of Mechanical Engineers, Fairfield, NJ, 1996, pp. 101–108.

[23]Tan, Z., and Howell, J. R., "A New Numerical Method for Radiation Heat Transfer in Nonhomogeneous Participating Media," *Journal of Thermophysics and Heat Transfer*, Vol. 4, No. 4, 1990, pp. 419–424.

[24]Lathrop, K. D., and Carlson, B. G., "Discrete-Ordinates Angular Quadrature of the Neutron Transport Equation," Los Alamos Scientific Lab., Rept. LASL-3168, Los Alamos, NM, Sept. 1964.

[25]Thurgood, C. P., Pollard, A., and Becker, H. A., "The Tn Quadrature Set for the Discrete Ordinates Method," *Journal of Heat Transfer*, Vol. 117, No. 4, 1995, pp. 1068–1070.

[26]Murthy, J. Y., Mathur, S. R. and Lim, C. K., "Automotive Applications of a Finite Volume Method for Radiative Heat Transfer," FEDSM 98, 1998 ASME International Fluids Engineering Div. Summer Meeting, American Society of Mechanical Engineers, Fairfield, NJ, 1998.